Available online at www.sciencedirect.com
SCIENCE DIRECT
Polymer 46 (2005) 539–552
polymer
www.elsevier.com/locate/polymer

Development of a unified framework for calculating molecular weight distribution in diffusion controlled free radical bulk homo-polymerization

G.D. Verros[a,*], T. Latsos[a], D.S. Achilias[b]

[a]Department of Electrical Engineering, Technological and Educational Institute (TEI) of Lamia, GR-35100 Lamia, Greece
[b]Laboratory of Organic Chemical Technology, Department of Chemistry, Aristotle University of Thessaloniki, GR-54006 Thessaloniki, Greece

Received 25 August 2004; received in revised form 14 November 2004; accepted 15 November 2004

Abstract

In the present work, two different approaches to model diffusion controlled free radical polymerization, namely the free volume model and the entanglement theory are compared. These approaches are applied to methyl methacrylate bulk polymerization in a batch reactor to calculate the conversion, total radical concentration, the number and weight average molecular weights as well as the entire molecular weight distribution as a function of the polymerization time and the process conditions. All the diffusion-controlled phenomena were taken into account, including gel, glass and cage effects as well as residual termination. The molecular weight distribution is calculated by direct numerical integration of a large system of non-linear ordinary differential equations describing the conservation of the mass of macromolecular species in the batch reactor. Model predictions are in good agreement with available experimental data for conversion, number and weight average molecular weights as well as the entire molecular weight distribution, thus justifying the ability of these models to describe the main issues of the diffusion-controlled free radical polymerization.

Keywords: Molecular weight distribution; Gel effect; Mathematical modeling

1. Introduction

The bulk free radical homo-polymerization is a process of major financial and scientific interest. The main characteristic of the process is the existence of diffusion-controlled reactions at high conversion. More specifically, besides the conventional chemical kinetics of free radical polymerization, physical phenomena related to the diffusion of various reactants play an important role in the polymerization process by directly influencing monomer conversion history and the product end-use properties.

Reactions that are influenced by diffusion phenomena include the termination of radicals, the growth of live polymer chains (propagation reaction), and the chemical initiation reaction. These reactions are related to the well known phenomena of the gel effect, the glass effect and the cage effect.

The gel effect or Trommsdorff–Norrish effect [1,2] has been attributed to the decrease in termination rate constants caused by a decrease in the mobility of polymer chains. In the early stages of polymerization, the termination kinetic rate constant is equal to the intrinsic constant k_{t0}, defined as the termination rate constant at zero conversion and involving two short chains. As time proceeds, the polymer concentration increases and the termination reactions become diffusion controlled. This leads to a decrease in termination rate constants followed by a sharp increase in polymer concentration. This auto-acceleration phenomenon strongly affects the end-use properties of the produced polymer as it leads to broader molecular weight distribution.

The glass effect is related to the decrease in the propagation rate constant caused by a decrease in the mobility of monomer molecules due to the 'freezing' of the reaction mixture at the glass transition temperature. More specifically, at a given high conversion, the polymerization

* Corresponding author. Address: P.O. Box 454, Plagiari, GR-57500 Epanomi, Greece. Tel.: +30 697 272 2651; fax: +30 223 102 2465.
E-mail addresses: gdverros@otenet.gr (G.D. Verros), verros@vergi-na.eng.auth.gr (G.D. Verros).

0032-3861/$ - see front matter © 2004 Elsevier Ltd. All rights reserved.
doi:10.1016/j.polymer.2004.11.025

temperature is equal to the glass transition temperature of the reaction mixture. As a consequence, glass transition occurs and the mobility of monomer molecules decreases causing a further decrease in the propagation rate constant.

The cage effect is strongly related to the physical and transport properties of the reaction mixture. As the initiator decomposes, only a fraction of the fragments escape from their 'cages' and react with the monomer to form primary radicals. This phenomenon affects not only the initiator efficiency but also the monomer conversion and the final product molecular weight distribution.

During the past 40 years, many models [3–38] with varying degrees of complexity have been published to describe the onset of the gel effect, monomer conversion as well as molecular weight developments in the polymerization reactor. These models can be classified in two main categories: entanglement and free volume models.

The entanglement models, based on the reptation theory of a polymer chain [39–42], show that the termination rate constant depends on the chain length of individual polymer chains. The free volume approach is based on the Vrentas–Duda equation [43,44] for the self-diffusion of a chain in a polymer solution.

In the past, doubts about both approaches have been raised in the literature. For example, O'Neil et al. [33] conducted experiments to examine the gel effect in free radical polymerization and raised doubt about the model based on entanglement arguments. In addition, several investigations [7,12,18] have raised doubts about the models based on free volume theory.

The aim of our work is to eliminate the shortcomings of the previous models and re-examine the ability of both approaches to describe diffusion controlled polymerizations. This could be achieved by developing a unified framework with respect to the physics of the process and comparing the predictions of both models for conversion history and molecular weight developments in the reactor as a function of the process conditions.

Regarding the calculation of the molecular weight developments in the reactor, models assuming that the kinetic rate constants are independent of individual chain length could be based on the method of moments [45–49] which allows the calculation of some characteristic averages of molecular weight distribution such as the number and the weight average of molecular weights. Several mathematical techniques have been proved effective in calculating the entire molecular weight distribution (MWD) in the presence of the gel effect assuming that the kinetic rate constants are independent of the chain length. These techniques include the statistical approach [50–57], the instantaneous molecular weight method [58–64], z-transforms [65,66], the method of moments [67–70], numerical fractionation [71], deconvolution techniques [72] and the direct numerical integration method [45,73–75]. However, to calculate the average molecular weights or the entire molecular weight distribution in the case of the chain length dependent termination one has to resort to the Galerkin finite element method [76–81] or to weighted residuals [82–85].

In the present work, the numerical integration method [45,73–75] is applied in both free the volume approach and the entanglement model. The methyl methacrylate diffusion-controlled bulk homo-polymerization in a batch reactor has been chosen as a working example. In what follows, the kinetic mechanism of methyl methacrylate polymerization is described, the corresponding polymerization rate functions are derived, the free volume approach as well as the entanglement theory is reviewed and a novel methodology for calculating MWD in the presence of chain length dependent termination is presented. Finally, results are presented and conclusions are drawn.

2. Kinetic mechanism and polymerization rate functions

The kinetic mechanism of methyl methacrylate (MMA) free radical polymerization includes the following elementary reactions:

Initiator decomposition

$$\mathrm{I} \xrightarrow{k_\mathrm{d}} 2\mathrm{R}_0$$

Chain initiation

$$\mathrm{R}_0 + \mathrm{M} \xrightarrow{k_\mathrm{Ii}} \mathrm{R}_1$$

Propagation

$$\mathrm{R}_n + \mathrm{M} \xrightarrow{k_\mathrm{p}} \mathrm{R}_{n+1}$$

Termination by combination

$$\mathrm{R}_n + \mathrm{R}_m \xrightarrow{k_{\mathrm{tc},n,m}} \mathrm{P}_{n+m}$$

Termination by disproportionation

$$\mathrm{R}_n + \mathrm{R}_m \xrightarrow{k_{\mathrm{td},n,m}} \mathrm{P}_n + \mathrm{P}_m$$

Chain transfer to monomer

$$\mathrm{R}_n + \mathrm{M} \xrightarrow{K_\mathrm{tm}} \mathrm{P}_n + \mathrm{R}_1$$

where I represents the initiator, M the monomer, R_n and P_n

stand for the live (free radicals) and the 'dead' polymer having n monomer units, respectively.

In the present work, the propagation rate constant was assumed independent of the chain length. Recent experiments [38] show that the propagation rate constant can depend on the chain length for low degrees of polymerization.

Based on the above mechanism, a large set of non-linear ordinary differential equations is derived to describe the mass conservation of the various reactants G in a well stirred batch polymerization reactor:

$$\frac{\mathrm{d}(V_\mathrm{G})}{\mathrm{d}t} = V r_\mathrm{G}; \quad V = V_0(1+\varepsilon X) \tag{1}$$

where V is the volume of the reacting mixture, t, the polymerization time, r_G represents the rate functions of the reactant present in the reactor, V_0, the volume of the reacting mixture at $t=0$, ε stands for linear contraction factor and X represents the monomer conversion.

r_{R_n} and r_{P_n} denote the net rates of the production of live radicals and dead polymer molecules, respectively. By combining the reaction rates of the various elementary reactions describing the generation and consumption of live and dead polymer molecules we can obtain the following expressions for the univariate chain length distribution (NCLD) [4,13]:

$$\begin{aligned} r_{\mathrm{R}_n} &= (k_\mathrm{I}[\mathrm{R}_0][\mathrm{M}] + k_\mathrm{tm}[\mathrm{M}]\lambda_0)\delta(n-1) + k_\mathrm{p}[\mathrm{M}] \\ &\quad \times([\mathrm{R}_{n-1}] - [\mathrm{R}_n]) - k_\mathrm{tm}[\mathrm{M}][\mathrm{R}_n] - [\mathrm{R}_n] \\ &\quad \times \sum_{m=0}^{\infty}(k_{\mathrm{td},n,m} + k_{\mathrm{tc},n,m)})[\mathrm{R}_m] \end{aligned} \tag{2}$$

$$\begin{aligned} r_{\mathrm{P}_n} &= k_\mathrm{tm}[\mathrm{M}][\mathrm{R}_n]\lambda_0 + \frac{1}{2}\sum_{r=1}^{n-1} k_{\mathrm{tc},n,-r,r}[\mathrm{R}_r][\mathrm{R}_{n-r}] \\ &\quad + [\mathrm{R}_n]\sum_{m=0}^{\infty} k_{\mathrm{td},n,m}[\mathrm{R}_m] \end{aligned} \tag{3}$$

where δ is Kronecker's delta and

$$\lambda_0 = \sum_{n=0}^{\infty} \mathrm{R}_n$$

is the total free radical concentration The termination by combination terms in the above equations have been written in accordance with the US definition in the field [4,13,45,86].

By assuming that the termination rate constants are independent of the chain length, the above equations can be simplified further [45–49]:

$$\begin{aligned} r_{\mathrm{R}_n} &= (k_\mathrm{I}[\mathrm{R}_0][\mathrm{M}] + k_\mathrm{tm}[\mathrm{M}]\lambda_0)\delta(n-1) \\ &\quad + k_\mathrm{p}[\mathrm{M}]([\mathrm{R}_{n-1}] - [\mathrm{R}_n]) - k_\mathrm{tm}[\mathrm{M}][R_n] \\ &\quad - (k_\mathrm{td} + k_\mathrm{tc})[\mathrm{R}_n]\lambda_0 \end{aligned} \tag{4}$$

$$r_{\mathrm{P}_n} = k_\mathrm{tm} M[\mathrm{R}_n]\lambda_0 + \frac{1}{2}k_\mathrm{tc}\sum_{r=1}^{n-1}[\mathrm{R}_r][\mathrm{R}_{n-r}] + k_\mathrm{td}\lambda_0[\mathrm{R}_n] \tag{5}$$

where k_tc and k_td are the termination rate constants for combination and disproportionation. The kinetic rate constants (k_tc, k_td, k_p, k_tm) in the above equations are assumed to be a function of the reaction mixture properties (conversion, number average molecular weight ($\bar{M}_\mathrm{n}$), weight average molecular weight ($\bar{M}_\mathrm{w}$)) but independent of the individual chain degree of polymerization.

According to Ray and co-workers [45,46] the leading moments of the univariate number chain length distribution (NCLD) associated with live and dead polymer chains are defined as:

$$\lambda_k = \sum_{n=1}^{\infty} n^k R_n; \quad \mu_k = \sum_{n=1}^{\infty} n^k P_n \tag{6}$$

The corresponding reaction rates for the moments can be obtained from Eqs. (4) and (5) by multiplying each term by n^k and adding over the total variation of n. The final equations for the moment rate functions are [45–49]:

$$\begin{aligned} r_{\lambda_\kappa} &= (k_\mathrm{I}[\mathrm{R}_0][\mathrm{M}] + k_\mathrm{tm}[\mathrm{M}]\lambda_0)\delta(k) \\ &\quad + k_\mathrm{p}[\mathrm{M}]\left[\sum_{i=0}^{k}\binom{k}{i}\lambda_i - \lambda_k\right] - (k_\mathrm{tc}\lambda_0 + k_\mathrm{td}\lambda_0 \\ &\quad + k_\mathrm{tm}[\mathrm{M}])\lambda_k, \\ r_{\mu_{kl}} &= (k_\mathrm{td}\lambda_0 + k_\mathrm{tm}[\mathrm{M}])\lambda_k + \frac{1}{2}k_\mathrm{tc}\sum_{i=0}^{k}\binom{k}{i}\lambda_i\lambda_{k-i} \end{aligned} \tag{7}$$

Combining the above reaction rates with the reactor design equation (Eq. (1)) results in a low order non-linear system that is solved numerically. The number average molecular weight ($\bar{M}_\mathrm{n}$) and the weight average molecular weight ($\bar{M}_\mathrm{w}$) are given as a function of the leading moments:

$$\bar{M}_\mathrm{n} = \mathrm{MW}\frac{(\mu_1+\lambda_1)}{(\mu_0+\lambda_0)}; \quad \bar{M}_\mathrm{w} = \mathrm{MW}\frac{(\mu_2+\lambda_2)}{\mu_1+\lambda_1} \tag{8}$$

where MW is the monomer molecular weight.

The mass balances for the initiator, the monomer and the primary radicals (R_0) are given in standard references [87].

3. Modeling diffusion controlled reactions

DeGennes [39–42] considered the effect of topological constraints imposed upon the motion of a polymer molecule by its neighbors. In his view the motion of a given

macromolecule is confined within a virtual 'tube' defined by the locus of its intersections (or points of 'entanglement') with adjacent molecules. The molecule is constrained and wriggles, snakelike along its own length by curvilinear propagation of length defects such as kinks or twists along the tube. This mode of motion was termed reptation. In the absence of significant polymer–polymer friction (the semi-dilute regime), application of scaling analysis in the context of the reptation model leads to the following law for the self-diffusion coefficient $D_{s,n}$:

$$D_{s,n} \sim n^{-2}c^{-7/4} \quad c^{**} > c > c^*, \quad n > N_c \tag{9}$$

where c is the polymer concentration, n the chain length of the macromolecules and c^*,$c^{**}$and N_c stand for critical concentrations and a critical chain length, respectively.

Based on Vrentas and Duda free volume theory [43,44] one can derive the following equation to describe the concentration and temperature dependence of the macromolecular mean self-diffusion coefficient in a polymer solution:

$$\bar{D}_p = (D_{p0}/\bar{M}^{\xi})\exp\lfloor -\gamma(\omega_m \bar{V}_m^* + \omega_p \bar{V}_p^* \xi_{13})/(V_f \xi_{13}) \rfloor \tag{10}$$

where $\bar{M}$ represents the mean molecular weight of the diffused species, ξ is an appropriate number, ω stands for weight fraction, subscripts p and m represent the dead polymer and the monomer, respectively. Other equation parameter values for methyl methacrylate polymerization, as a function of temperature and concentration, have been tabulated by Achilias and Kiparissides [20].

It should be noted here that there is a variety of laws describing the molecular weight dependence of the macromolecular mean self diffusion coefficient in a diffusion-controlled polymerization. For example, according to Marten and Hamielec [7] ξ is equal to 1.75 and $\bar{M}$ represents the dead polymer cumulative weight average molecular weight. Soh and Sundberg [14–17] used an exponent $\xi = 3.4$ and suggested that $\bar{M}$ is equal to the instantaneous chain length of the live polymer. Achilias and Kiparissides [21] suggested that $\xi = 2$ and $\bar{M}$ is equal to the dead polymer cumulative weight average molecular weight. In the present work, $\bar{M}$ stands for the number average degree of polymerization weight of the live polymer and the exponent ξ is set equal to 2 according to the reptation model [13].

It is believed that several investigations [7,12,18] have raised doubts about the ability of free volume models to describe diffusion controlled polymerizations due to the application of different laws describing the molecular weight dependence of the macromolecular mean self diffusion coefficient.

Regarding the doubts raised [33] about the ability of the entanglement theory to predict the gel effect one could anticipate that a complete entanglement theory should account not only for the dead polymer entanglements but also could take into account the effect of the entanglements on the diffusion of the live polymer. Actually, a complete theory could apply the free volume approach to predict the effect of the entanglements on the diffusion of the live polymer. This task is beyond the scope of the present work.

To account for the segmental diffusion of the radical chains, the self-diffusion coefficient is multiplied by a factor F_{seg} [88]. Therefore, the effective diffusion coefficient is given by

$$\bar{D}_{pe} = F_{seg}\bar{D}_p \tag{11}$$

To express the overall termination kinetic rate constant k_t ($k_t = k_{tc} + k_{td}$) in terms of the free radical self-diffusion coefficient, most free volume models utilized the Smoluchowski equation [89]:

$$\frac{1}{k_t} = \frac{1}{k_{t0}} + \frac{1}{4\pi N_A r_t \bar{D}_{pe}} = \frac{1}{k_{t0}} + \frac{r_t^2 \lambda_0}{3\bar{D}_{pe}} \tag{12}$$

where N_A is the Avogadro number, k_{t0} stands for the intrinsic termination rate constant defined at zero conversion and involving two short chains, $\lambda_0 (= 1/((4/3)N_A \pi r_t^3))$ is the total concentration of live radicals (Eq. (11) in Ref. [4]) r_t represents the effective reaction radius for the termination reaction calculated either from the live radicals equation $r_t = (1/((4/3)N_A \pi \lambda_0))^{1/3}$ or by the excess chain end mobility theory [14,20,21]. Both approaches give similar results.

The Smoluchowski equation was also utilized to describe the variation of the termination kinetic rate constants in the entanglement theory [13,78]:

$$\begin{aligned} k_t &= k_t \quad c < c^* \\ k_{t,n,m} &= 4\pi N_A r_t (D_{s,n} + D_{s,m}) = C4\pi N_A r_t c^{-7/4}(n^{-2} + m^{-2}) \\ &\quad c > c^*, \quad n, m > N_c \end{aligned} \tag{13}$$

The above equation can be further recast to include the critical chain length N_c, defining the semi-dilute region in the entanglement theory [78]:

$$k_{t,n,m} = C4\pi N_A r_t c^{-7/4}[(n + N_c)^{-2} + (m + N_c)^{-2}], \quad c > c^* \tag{14}$$

Following Tirrell and co-workers [78], the value of the proportionality constant C was calculated by assuming

$$k_{t,1,1} = k_{t0} \quad \text{at} \quad c = c^* \tag{15}$$

At very high conversion, the termination rate constants have to be corrected to account for the motion of the radical chains caused by the monomer propagation reaction. Schulz [3], Soh and Sundberg [17], Gilbert and co-workers [23] considered that, at very high conversion, the monomer propagation reaction contributes to the migration of the radical center, despite the actual translational immobility of

the polymer chain as a whole. This phenomenon is known as 'residual termination' or 'reaction diffusion'.

Many models were developed to account for the residual termination. [17,23] All models assume that the residual termination rate constant is proportional to the frequency of monomer addition to the radical chain end:

$$k_{t,reac} = Ak_p[M] \tag{16}$$

Finally, the overall termination rate constant is given by

$$k_{te} = k_t + k_{t,reac} \tag{17}$$

The cage effect was taken into account following Achilias and Kiparissides [21] model developments:

$$\frac{1}{f} = \frac{1}{f_0} + E\frac{r_2^3}{3r_1}\frac{k_{p0}}{f_0}\frac{[M]}{D_I} \tag{18}$$

where f_0 and f denote the initial initiator (at $t=0$) and the time-varying initiator efficiency, respectively. [M] stands for the monomer concentration, r_2 is equal to the initial hydrodynamic volume of the polymer, r_1 represents the diameter of MMA molecule and E is a proportionality constant treated as an adjustable parameter. k_{p0} is the propagation rate constant in the absence of diffusion limitations and D_I is the primary radical diffusion coefficient calculated directly by the Vrentas–Duda free volume correlation [21]:

$$D_I = D_{I0}\exp\lfloor -\gamma\bar{V}_I^*M_{jI}[(\omega_m/M_{jm}) + (\omega_p/M_{jp})]/V_f\rfloor \tag{19}$$

Finally, the glass effect was considered by taking into account diffusion limitations in the propagation reaction at high monomer conversion [18,21]

$$\frac{1}{k_p} = \frac{1}{k_{p0}} + \frac{1}{4\pi N_A r_m D_m} = \frac{1}{k_{p0}} + \frac{r_m^2\lambda_0}{3D_m}, \quad r_m = r_t \tag{20}$$

where r_m is the effective radius for propagation reaction set equal to the effective radius for termination r_t [21]. D_m is the self-diffusion coefficient of the monomer and can be calculated directly by the Vrentas–Duda free volume correlation as follows:

$$D_m = D_{m0}\exp[-\gamma(\omega_m\bar{V}_m^* + \omega_p\bar{V}_p^*\xi_{13})/V_f] \tag{21}$$

Values of Eqs. (18)–(21) parameters for the methyl methacrylate polymerization are given in full detail elsewhere (Table 1 in Ref. [21]).

4. Calculation of molecular weight distribution

The method of direct integration was applied to calculate the molecular weight distribution for methyl methacrylate bulk homo-polymerization in a well stirred batch reactor. According to this method the Eqs. (2)–(5) describing the conservation of macromolecular species in the reactor are solved by standard integration techniques.

As a critical point appears at the c^* in the entanglement models, a 4th order Runge–Kutta integration method with a varying time step was used. [90,91]. This integration method is particularly effective in the treatment of critical points and allows a simultaneous solution of the initiator and monomer mass balances along with the macromolecular species mass balances.

A detailed methodology to calculate MWD in the case of termination kinetic rate constants independent of the chain length is given in our previous work [75]. The present work focuses on the case of chain length dependent termination. In order to increase computational efficiency and decrease the required time for execution two well established assumptions were implemented: (a) the quasi steady state approximation (QSSA) for the live polymer radicals and (b) the continuous variable approximation (CVA).

To reduce execution time for the solution of the problem we have to resort to quasi-steady approximation (QSSA). Hamielec and co-workers [92–95] successfully implemented this assumption to calculate MWD by the instantaneous MWD method in linear polymerization with diffusion controlled termination reactions. According to the QSSA the rate of variation with time of live radical concentration, is relatively small, compared to the other terms of Eq. (1). Consequently, the first term of reactor design equation drops for live radical mass balances and these equations are transformed to a highly coupled algebraic system, ($r_{R_n} = 0$) which is solved numerically in order to calculate live radical MWD.

The continuous variable approximation (CVA) was implemented to decrease the number of equations of the algebraic live radical mass balance system. The CVA introduced by Bamford and Jenkins [96], Zeman and Amundson [76,77] was utilized in many works [78–81] dealing with the calculation of MWD in free radical homopolymerization with diffusion limited termination. By applying the CVA the discrete system is transformed to a continuous variable system by expanding the concentration of live radicals having chain length L, in Taylor expansion truncated after the second term:

$$[R_{n-1}] = [R_n] - \frac{\partial[R]}{\partial x}\Big|_{x=n} + \frac{1}{2}\frac{\partial^2[R]}{\partial x^2}\Big|_{x=n} \tag{22}$$

The derivatives in the above expression can be directly calculated by using a finite difference scheme significantly reducing the number of equations to be solved:

$$\frac{\partial[R]}{\partial x}\Big|_{x=n} = \frac{([R_n] - [R_{n-\eta step}])}{\eta step};$$
$$\frac{\partial^2[R]}{\partial x^2}\Big|_{x=n} = \frac{([R_n] - 2[R_{n-\eta step}] + [R_{n-2\eta step}])}{\eta_{step}^2} \tag{23}$$

where ηstep is the chain length step used in the discretization.

Implementation of CVA reduces the number of mass balances of live radicals to be solved and transforms them to an ordinary differential equations system with respect to chain length that can be directly solved using the finite difference scheme of Eqs. (22) and (23).

More specifically, the live radicals mass balances (Eq. (2)) become time invariant equations ($r_{R_n} = 0$) by applying QSSA. These equations, by introducing the expanded live radical concentration in a Taylor series (Eqs. (22) and (23)), are expressed in the following form:

$$\begin{aligned}&(k_i R_0[M] + k_{tm}[M]\lambda_0]\delta(n-1)\\&-k_{tm}[M]R_n - k_p[M]\frac{([R_n]-[R_{n-\eta step}])}{\eta step}\\&+\frac{1}{2}k_p[M]\frac{([R_n]-2[R_{n-\eta step}]+[R_{n-2\eta step}])}{\eta_{step}^2}\\&-[R_n]\sum_{m=0}^{\infty}(k_{td,n,m}+k_{tc,n,m})[R_m]=0\end{aligned} \tag{24}$$

The main difficulty in calculating MWD for live radicals arises from the calculation of summations appearing in the termination by combination and disproportionation reaction rates (see Eq. (24)). By substituting Eq. (14) into the summation

$$\sum_{m=0}^{\infty}(k_{td,n,m}+k_{tc,n,m})R_m$$

Eq. (24), the following relation is derived:

$$\begin{aligned}&\sum_{m=0}^{\infty}(k_{td,n,m}+k_{tc,n,m})R_m\\&=\sum_{m=0}^{\infty}C4\pi N_A r_t c^{-7/4}[(n+N_c)^{-2}\\&\quad+(m+N_c)^{-2}]R_m\\&=C4\pi N_A r_t c^{-7/4}(n+N_c)^{-2}\lambda_0+S_0\end{aligned} \tag{25}$$

where S_0 stands for the summation

$$\sum_{m=0}^{\infty}C4\pi N_A r_t c^{-7/4}(m+N_c)^{-2}[R_m];\quad \lambda_0=\sum_{n=0}^{\infty}R_n$$

represents the free radical total concentration.

Accordingly, the calculation of the MWD in the case of the chain length dependent termination includes the following steps:

(i) assume a value for the live radical total concentration λ_0.
(ii) assume a value for the summation S_0.
(iii) calculate the entire MWD for live radicals by directly solving Eq. (24).
(iv) calculate the summation S_0.
(v) assume this value for S_0 and repeat steps (ii)–(iv) till the calculated value and the assumed one for S_0 agree within a tolerance.
(vi) given the MWD calculate the live radical total concentration λ_0.
(vii) assume this value for λ_0 and repeat steps (i)–(vi) till the calculated value and the assumed one for the live radical total concentration agree within a tolerance.
(viii) Calculate the discrete summations

$$\frac{1}{2}\sum_{r=1}^{n-1}k_{tc,n,-r,r}R_nR_{n-r},\ R_n\sum_{m=0}^{\infty}k_{td,n,m}R_m$$

transformed to integrals by using the 7-point Newton–Cotes integration rule, where 'infinity' is replaced by a very large number.
(ix) calculate MWD for the dead polymer by solving macromolecular mass balances (Eq. (3)) with a varying step 4th order Runge–Kutta method.

This algorithm could be extended in the case of propagation chain length dependent polymerization without any difficulty.

By applying the above methodology one can directly calculate dead polymer normalized weight molecular weight distribution (WMWD) defined as

$$\sum_{i=1}^{\infty}nP_n/X$$

where X is the monomer conversion.

5. Results and discussion

The model of Achilias and Kiparissides [21], and the model of Tuling and Tirrell [13,78] were utilized as representative models of the free volume approach and the entanglement theory, respectively. Achilias and Kiparissides model is based on the method of moments and utilizes the Vrentas–Duda equation for the self diffusion coefficient (Eq. (10)) along with the Smoluchowski equation (Eq. (12)), to calculate termination kinetic rate constants as a function of polymer concentration, temperature and dead polymer weight average molecular weight ($\bar{M}_w$). It should be noted that in the original model $\bar{M}$ (see Eq. (10)) represents the weight average molecular weight of the dead polymer and in the present model $\bar{M}$ stands for the number average degree of polymerization of the live polymer. This leads to a significant improvement in agreement between model predictions for number and weight average molecular weights and experimental data.

The Tirrell and co-workers model [13] is based on the reptation theory (Eq. (9)) and the Smoluchowski equation (Eq. (13)) is utilized to calculate diffusion controlled

termination rate constants in terms of polymer concentration and individual macromolecule chain length.

Both models account not only for the gel effect but also for residual termination, the glass effect and the cage effect by introducing in each model the appropriate equations as described in previous sections.

Following Achilias and Kiparissides [21] the adjustable parameters for the free volume approach include the quantities $D_{p0}F_{seg}$ (see Eqs. (10) and (11)), D_{m0} (see Eq. (21)), E/D_{I0} (see Eqs. (18) and (19)). Additionally, following Tirrell and co-workers [78] the residual termination was treated as an adjustable quantity by introducing the parameter A (Eq. (16)) in the estimation procedure.

The entanglement model has as adjustable quantities, the parameter c^* (Eq. (14)), D_{m0} (Eq. (21)), E/D_{I0} (Eqs. (18) and (19)) and the parameter A (Eq. (16)). It was found convenient to define c^* in terms of the critical monomer conversion X_c, accounting for the onset of the gel effect.. The parameter N_c was found to have very little effect on the predicted values for monomer conversion, number and weight average molecular weight [78]. Consequently, this quantity was not added in the estimation procedure and its value remains constant in all numerical experiments ($N_c = 0$).

Values for the physical constants of the reactant mixture used in our numerical experiments (kinetic rate constant for initiator decomposition, $k_p/k_t^{0.5}$, k_{tm}/k_p, physical properties, etc) are given in full detail elsewhere (Table 1, Ref. [21]). The initiator efficiency was set equal to 0.63. This value for the initiator efficiency is in good agreement with the reported value (0.58) by Achilias and Kiparissides [21]. For the propagation rate constant the reported values of Beuermann et al. [32] were utilized.

The adjustable parameters of both models were estimated by fitting models predictions to experimental data of conversion history, number and weight average molecular weights versus time, as well as total free radical concentration at different polymerization time. The reaction conditions and the experimental data of Hamielec and co-workers [97,98] were employed. They use AIBN at various concentrations as the initiator in their isothermal experiments and the polymerization temperature was from 50 to 90 °C. Moreover, they represent the weight molecular weight distribution (WMWD) obtained in their experiments by GPC as an exponential function:

$$\text{Normalized WMWD} = \exp(A_0 + B_0X + C_0X^2 + D_0X^3) \tag{26}$$

where X is the monomer conversion, the parameters A_0, B_0, C_0, D_0 are given as a function of polymerization temperature and initiator feed concentration in their original work [97].

In the parameter estimation procedure for the free volume approach the number and weight average molecular weights were calculated by using the leading moments balances (Eqs. (7) and (8)). Then, the entire MWD was calculated by introducing into the model the previously estimated adjustable parameters and using the direct numerical approach [75].

In the entanglement model the number and weight molecular weight were calculated by solving the entire MWD. In this case the leading moments for the dead polymer NCLD were calculated by using their definition (Eq. (6)) Similar results for the predicted WMWDs by the reptation theory were shown by Tirrell and co-workers [78]. The difference between their original work [78] and the present model is the inclusion of the glass effect and the cage effect in addition to the gel effect. Moreover, these researchers used the Galerkin Finite Element Method (GFEM). This method is a powerful tool for solving complex scientific problems appearing in the Computational Transport Phenomena but the inclusion of integrals in the governing equations such as the termination by combination reaction rates in our case, significantly increases the computational time as it requires the inversion of a large non-sparse matrix by full Gaussian elimination [99,100]. The authors are also aware that more sophisticated algorithms based on discrete residuals are available in the open literature [85]. The main advantage of the present method over these algorithms is simplicity in code construction and development based on standard mathematical methods. Please note, that the present method, due to the application of well established procedures in its development, could be used as a reference solution to check the validity of the other available methods in the open literature.

The method presented in this work is not only easily implemented in a computer code but is also simple and effective thus permitting the parameter estimation procedure with standard non-linear regression methods. The time step was automatically adjusted by the integration method resulting in a significant decrease in time required for computation. More specifically, the step doubling technique [91] was used to estimate the time step for integration. In this technique the optimal time step was estimated by taking each time-step twice, once as a full step and then independently as two half-steps. Each of the three separate Runge–Kutta steps in the procedure requires 4 evaluations, but the single and the double sequence share a starting point so the total is 11 evaluations. Regarding computational time spent in the calculation of the MWD with the entanglement model, each evaluation of the 4th order Runge–Kutta requires 7 s of real time in a computer equipped with a 2.66 GHz processor to solve simultaneously 4×10^4 equations ($n_{step} = 10$) describing the conservation of the macromolecular species in the reactor. Most computational time was spent in the calculation of the termination by combination summations appearing in the dead polymer mass balances (Eq. (3)); If the overall termination rate constant ($k_{t,n,m}$) is set equal to termination by the disproportionation rate constant ($k_{t,n,m} = k_{td,n,m}$, $k_{tc,n,m} = 0$)

the real time spent on calculations is reduced to 0.3 s per each Runge–Kutta evaluation.

The estimated parameters of both models are summarized in Table 1. The values for $F_{seg}D_{p0}$ decrease by increasing temperature and initiator feed concentration. As D_{p0} is a constant the results shown in Table 1 indicate that F_{seg} is a strong function of the process conditions and decreases by increasing temperature and initiator feed concentration.

In this work, the parameter D_{m0} is equal to 10^{-9}–10^{-8} cm^2/s (70 °C) and equal to 10^{-7}–10^{-6} cm^2/s (90 °C). Ju et al. [101,102] based on diffusion data measurements expressed this parameter for PMMA as a function of the absolute temperature T: $D_{m0} = D'_{m0}\, e^{-E_m/RT}$, where R is the universal gas constant, E_m is equal to 87.128 kJ/g mol and D'_{m0} is equal to 223.4 cm^2/s. Based on the above equation the calculated values of this parameter at the temperature range of interest are 1.17×10^{-11} cm^2/s (70 °C) and 6.3×10^{-11} cm^2/s (90 °C), respectively. This discrepancy is attributed to the fact that in Eq. (20) the effective radius for the propagation reaction was set equal to the effective radius for the termination reaction. This simplification could introduce some error in the estimated values of D_{m0}.

In Table 1, it is shown that the reactor conditions strongly influence parameter E and A. However, Russell et al. [23] reported for AIBN (0.3 wt%) initiated MMA polymerization at 70 °C an upper value for parameter A equal to 9.363 and a lower value equal to 0.7. Under the same polymerizing conditions Soh and Sundberg [17] reported a value equal to 5.846. The reason for this difference between theory predictions [17,23] and present work is explained in the following paragraphs.

There is also a discrepancy between the values of E/D_{I0}, D_{m0} and A as predicted by the free volume and entanglement theory attributed to inherent differences in their ability to predict experimental data at high polymer concentration. More specifically, the reptation scaling law for the concentration dependence of the self-diffusion coefficient (Eq. (9)) is not valid at high polymer concentration near the end of the polymerization where the polymer–polymer interactions are important. This leads to different estimated values for the glass effect, the cage effect and the residual termination parameters.

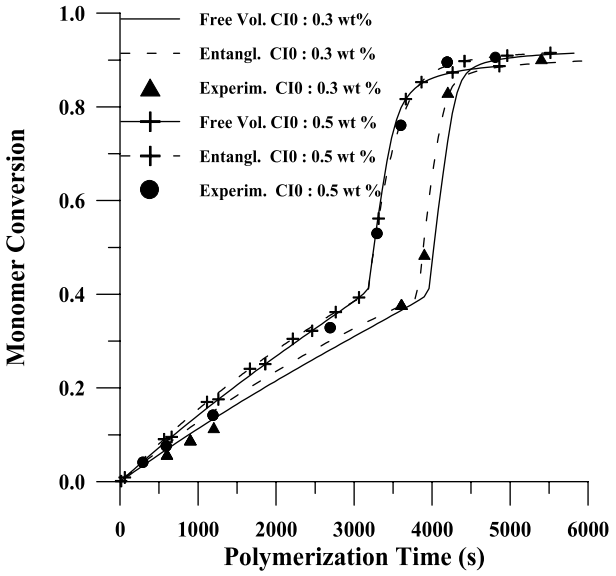

Fig. 1. Monomer conversion versus time for different initiator feed concentration (CI0). Polymerization temperature 70 °C. Experimental data from Balke and Hamielec [97].

Figs. 1–11 show the results of the numerical experiments for monomer conversion, total free radical concentration, number and weight average molecular weight as well as the MWD. Detailed descriptions of the diffusion phenomena effects on initiator efficiency, propagation and termination rate constants, the onset of gel and glass effects as well as their relation to monomer conversion, number and weight average molecular weights as well as total radical concentration for methyl methacrylate polymerization, have been given by many researchers in the field [1–38]. The present work focuses on comparing the ability of the different approaches in predicting the MWD as a function of the process conditions by using a simple and effective method.

Figs. 1–6 depict the monomer conversion history and the

Table 1
Estimated parameters

Free volume model					
Temperature (°C)	CI0 (%wt)	$F_{seg}D_{p0}$ (cm^2/s)	D_{m0} (cm^2/s)	E/D_{I0} (s/m^2)	A
70	0.3	0.06	10^{-8}	2.66	14.1
70	0.5	0.042	1.3×10^{-9}	47.86	31.21
90	0.3	0.019	2.2×10^{-6}	7.6	38.7
90	0.5	0.014	4.4×10^{-7}	2239	22.1
Entanglement model					
Temperature (°C)	CI0 (%wt)	X_c	D_{m0} (m^2/s)	E/D_{I0} (s/cm^2)	A
70	0.3	0.393	2×10^{-9}	1.04	14.6
70	0.5	0.414	2.8×10^{-9}	27.54	32.4
90	0.3	0.424	2.5×10^{-11}	2884	82
90	0.5	0.482	1.44×10^{-8}	43.15	52

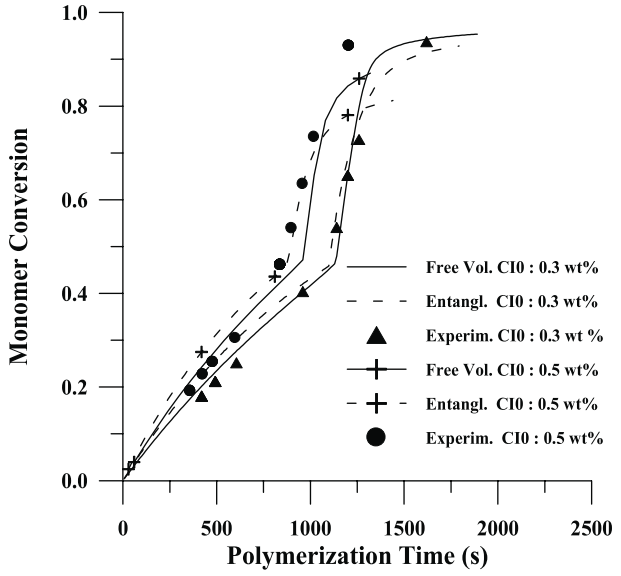

Fig. 2. Monomer conversion versus time for different initiator feed concentration (CI0). Polymerization temperature 90 °C. Experimental data from Balke and Hamielec [97].

average molecular weights for different polymerization temperatures and initiator feed concentrations as predicted by the free volume approach and the entanglement theory. A good agreement between experimental data and models predictions is observed. However, there is a discrepancy between experimental data and model predictions for monomer conversion and average molecular weights near the end of the polymerization. This discrepancy could be attributed to the non-isothermal conditions in the reactor after the onset of gel effect.

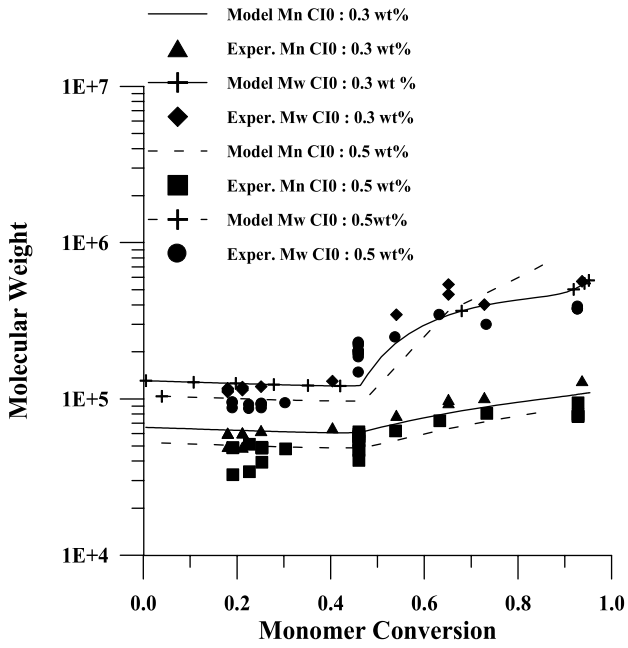

Fig. 4. Free volume model. Number and weight average molecular weight versus monomer conversion for different initiator feed concentration (CI0). Polymerization temperature 90 °C. Experimental data from Balke and Hamielec [97].

In both models, in the early stages of polymerization the overall kinetic rate constant for termination (k_t) remain almost equal to its intrinsic value k_{t0}. Consequently, the conversion increases almost linearly with polymerization time (Figs. 1 and 2) and the molecular weights remain almost constant (Figs. 3–6). However, at a given polymerization time depending on the reaction conditions (polymerization

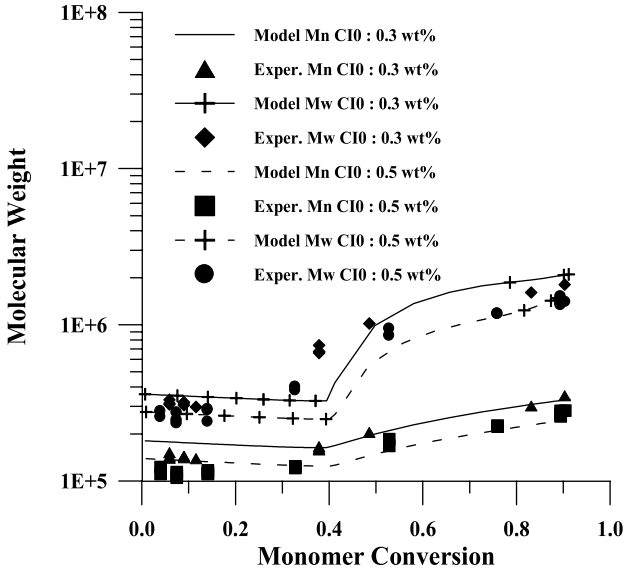

Fig. 3. Free volume model. Number and weight average molecular weight versus monomer conversion for different initiator feed concentration (CI0). Polymerization temperature 70 °C. Experimental data from Balke and Hamielec [97].

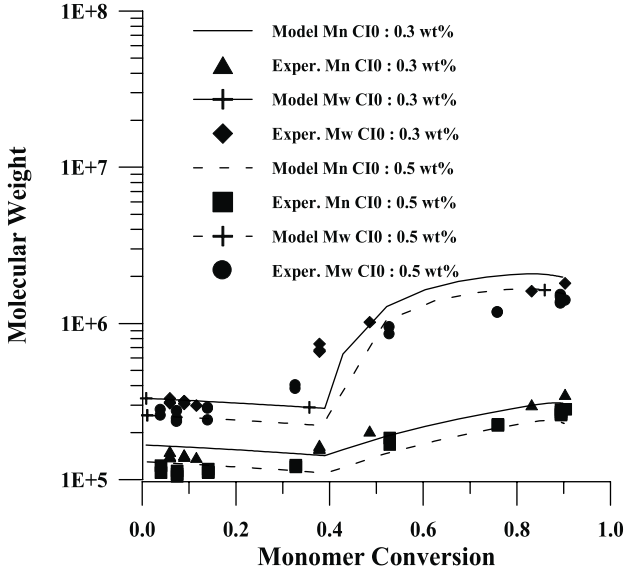

Fig. 5. Chain entanglement theory. Number and weight average molecular weight versus monomer conversion for different initiator feed concentration (CI0). Polymerization temperature 70 °C. Experimental data from Balke and Hamielec [97].

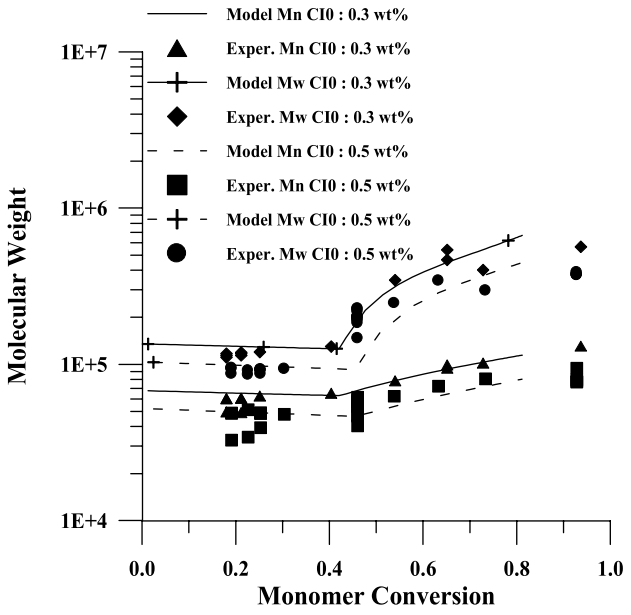

Fig. 6. Chain entanglement theory. Number and weight average molecular weight versus monomer conversion for different initiator feed concentration (CI0). Polymerization temperature 90 °C. Experimental data from Balke and Hamielec [97].

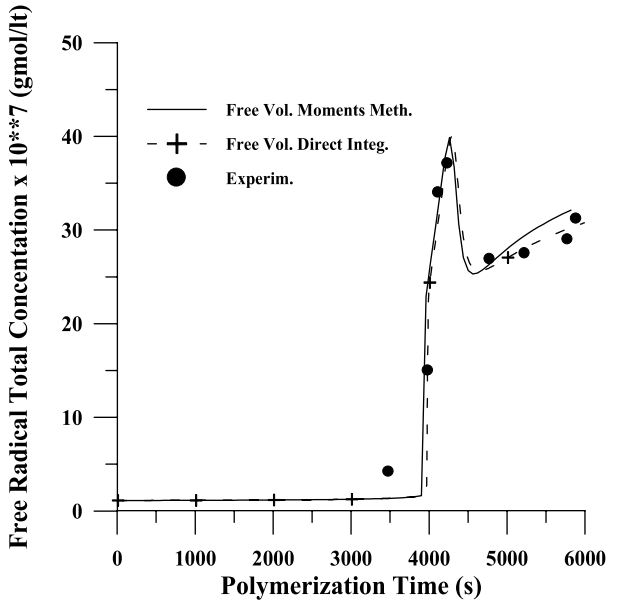

Fig. 7. Total free radical concentration versus time. Initiator feed concentration 0.3 wt%. Polymerization temperature 70 °C. Experimental data from Hamielec and co-workers [98].

temperature, initiator feed concentration) a sharp increase in monomer conversion and average molecular weight occurs due to the auto-acceleration phenomenon (gel effect). The onset of the gel effect in the free volume approach is a continuous function of the process conditions while in the reptation theory it is introduced as a critical point (X_c). Although these models are based on different physical grounds, both show a good ability to predict the

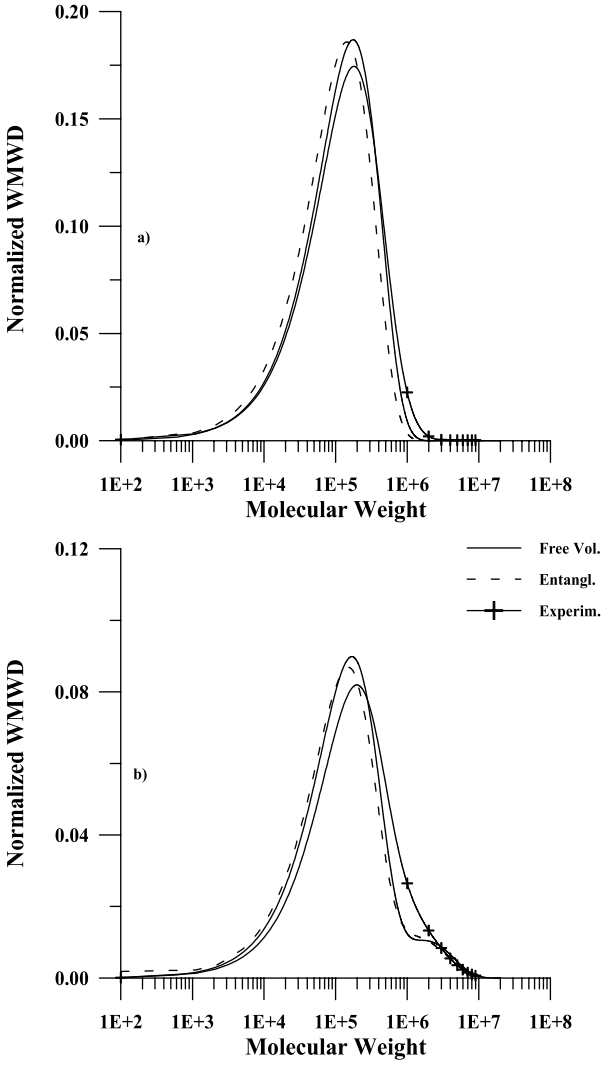

Fig. 8. Comparison of predicted weight molecular weight distribution with experimental data [97]. Polymerization temperature 70 °C. Initiator feed concentration 0.3 wt%. Polymerization time (a) 3600 s; (b) 5400 s.

experimental data as a function of the process conditions. This is attributed to the fact that both models follow the same fundamental law derived from the reptation theory [39–42] describing the effect of diffused species chain length on self-diffusion coefficient:

$$D_s \propto \frac{1}{n^2} \tag{27}$$

It should be noted here that this law is strictly valid in the semi-dilute region. The error introduced in the model by the extension of the above law to higher polymer concentrations where the polymer–polymer interactions are important could explain the observed discrepancy between the higher values of parameter A obtained in this work (Table 1) and the theory predictions.

Moreover, it is shown that the introduction of the radical number average molecular weight in Eq. (27) instead of individual species chain length is a reasonable assumption

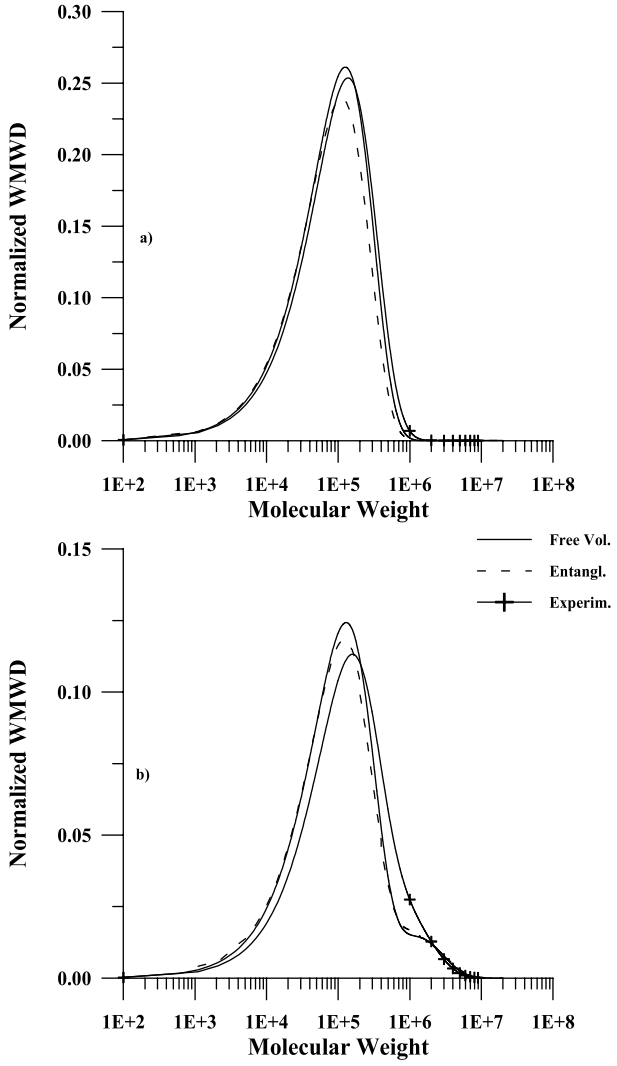

Fig. 9. Comparison of predicted weight molecular weight distribution with experimental data [97]. Polymerization temperature 70 °C. Initiator feed concentration 0.5 wt%. Polymerization time (a) 2700 s; (b) 4820 s.

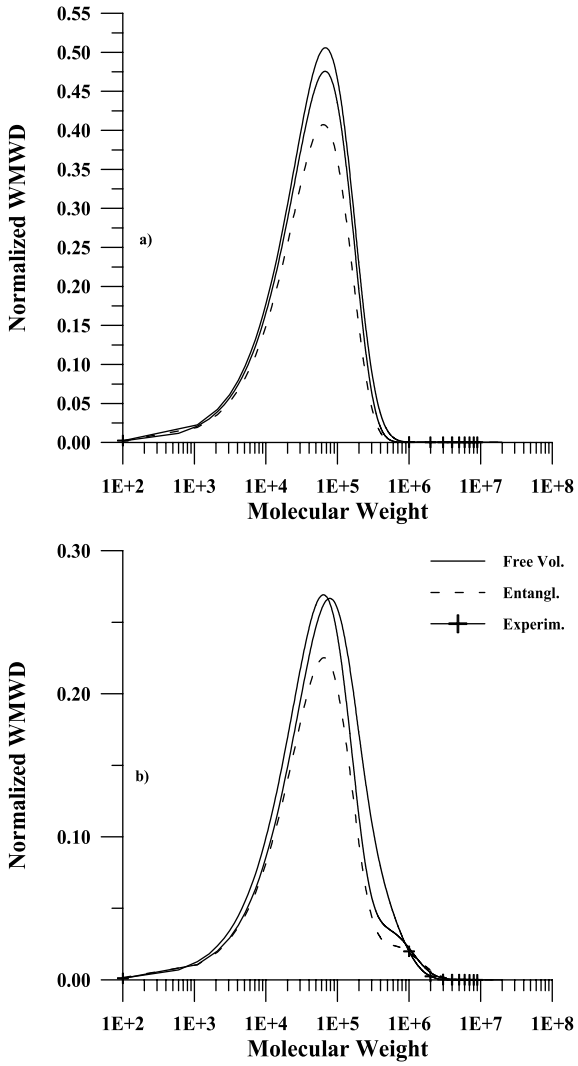

Fig. 10. Comparison of predicted weight molecular weight distribution with experimental data [97]. Polymerization temperature 90 °C. Initiator feed concentration 0.3 wt%. Polymerization time (a) 920 s; (b) 1620 s.

as in the case of the free volume approach. This is further supported by the fact that Tirrell and co-workers [13] obtained excellent results for monomer conversion history and average molecular weights by introducing in the fundamental reptation law (Eq. (9)) the radicals number average molecular weight instead of individual species chain length.

It should be noted here, that both models besides their similarities (same equations for the glass and the cage effect), have fundamental differences in the concentration dependence of the self-diffusion coefficient of live radicals (Eqs. (9) and (10)) However, it is expected that as the gel effect is controlled by the self-diffusion coefficient of live radicals and most of the dead polymer is produced during the gel effect, the entanglement theory and the free volume approach shall give completely different results for molecular weight developments and conversion history. However, the inclusion of the same scaling law for the molecular weight dependence of the live polymer self-diffusion coefficient leads to almost identical results regarding conversion history and molecular weight developments during the gel effect. This indicates that the molecular weight developments are crucial for the onset of the gel effect.

In Fig. 7 total free radical concentration as predicted by the free volume theory using the method of moments (Eqs. (7) and (8)) and the direct numerical integration method are compared with experimental data [98]. It should be noted here that in the method of moments the quasi steady state approximation (QSSA) was not made. The results shown in this figure justify completely the QSSA. The predicted total concentration of radicals (not shown) by using the entanglement theory was found to be in less satisfactory agreement with experimental data due to the simplification made in the calculation of the proportionality constant C (Eq. (15)).

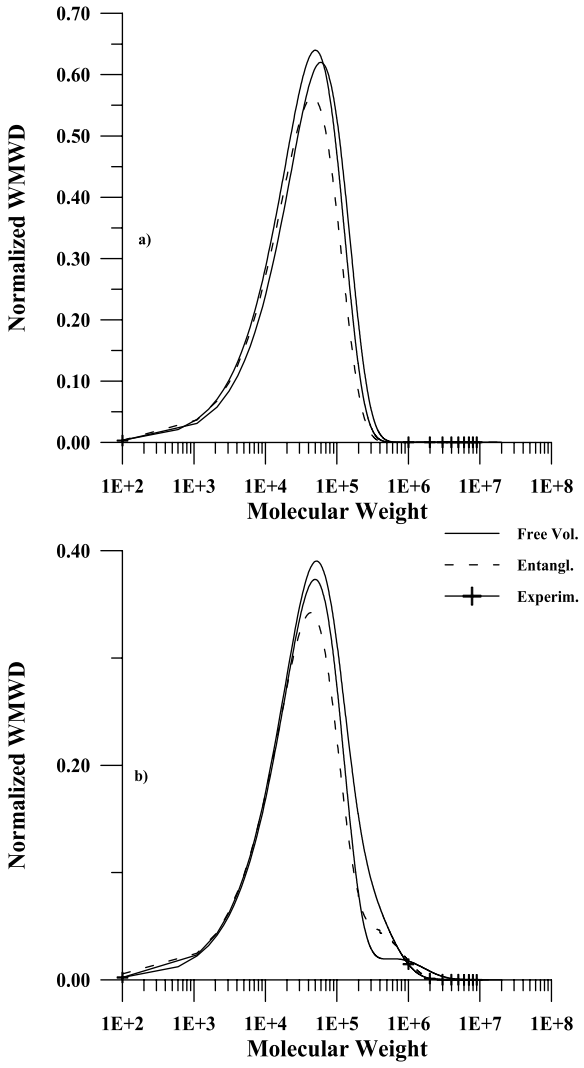

Fig. 11. Comparison of predicted weight molecular weight distribution with experimental data [97]. Polymerization temperature 90 °C. Initiator feed concentration 0.5 wt%. Polymerization time (a) 420 s; (b) 1206 s.

A deeper question arises from the results shown in the previous figures and the fact that an infinite number of distributions exist with the first three leading moments or in other words the number and weight average molecular weights being identical: How different are the predictions of the entanglement theory from the free volume approach for the polymer entire WMWD?

In Figs. 8–11 a good agreement is shown between WMWD predicted by the free volume approach and the entanglement theory using the direct numerical integration method. These results completely justify the ability of the entanglement model and the free volume approach to predict the diffusion controlled bulk polymerization of MMA.

As initiator concentration increases more radicals are produced thus leading to a decrease in average molecular weights (Figs. 3–6). In this case, the maximum of the WMWD increase and narrower distributions are obtained (Figs. 8–11). As polymerization temperature increases the WMWD maximum increases due to the increase in the termination kinetic rate constants and narrower distributions are obtained (Figs. 8–11).

In case A, the WMWD was calculated before the onset of the gel effect while in case B the WMWD was calculated near the end of polymerization. In Case A there are very weak diffusion limitations and the predicted WMWD is unimodal as predicted by most workers in the field [30,59,60,63]. In case B there are strong diffusion limitations and the predicted WMWDs are bimodal. This is attributed to the fact that after the onset of the gel effect the termination kinetic rate constants sharply decrease, allowing the production of radicals with higher molecular weights thus leading to broader molecular weight distribution. The observed discrepancy at the very high molecular weight range (8×10^5–2×10^6) between the experimental data of Balke and Hamielec [97] and the predictions of both models is attributed partially to the limited resolution of their GPC procedure at very high molecular weights reported in their original work as well as to the previously discussed physical limitations of the present models.

6. Conclusions

In the present work a unified framework is developed for modeling diffusion controlled free radical homo-polymerization. A novel methodology for calculating the entire MWD in the case of a complex reaction mechanism including chain length dependent termination was presented. This simple and effective algorithm is based on the direct numerical integration method of a large non-linear integro-differential equations system describing the conservation of the mass of the various reactants present in a batch polymerization reactor. In the development of this method two well-established assumptions, the quasi steady state approximation (QSSA) for live radicals and the continuous variable approximation (CVA), were made. The QSSA was further justified by comparing present algorithm predictions for total free radical concentration with results obtained by the method of moments without making any assumption.

All the physical phenomena related to diffusion controlled free radical polymerization such as the gel, the glass and the cage effects were taken into account. Moreover, two different approaches for modeling the gel effect, namely the entanglement theory and the free volume approach, were compared. These approaches, although based on completely different physical grounds, were shown to give almost identical results when they were applied to methyl methacrylate polymerization in a batch reactor. Both model predictions are in good agreement with experimental data for monomer conversion, total free radical concentration, number and weight average molecular weight, as well as the entire molecular weight distribution for different polymerization time. These results completely justify the

ability of both free volume and chain entanglement models despite their inherent differences, to describe the complex kinetics of MMA polymerization.

It is believed that the present work may be applied to other diffusion controlled polymerizations thus leading to a more rational design of industrial reactors.

Acknowledgements

G.D.V. is thankful to Ms K. Somerscales for her help in preparing the manuscript. The reviewers of this work are also acknowledged for their constructive comments.

References

[1] Norrish RGW, Smith RR. Nature (London) 1942;150:336–7.
[2] Trommsdorff E, Koble H, Lagally P. Makromol Chem 1948;1(3): 169–98.
[3] Schulz GV. Z Phys Chem (Frankfurt am Main) 1956;8:290–317.
[4] Benson SW, North AM. J Am Chem Soc 1962;84(6):935–40.
[5] Hui AW, Hamielec AE. J Appl Polym Sci 1972;16(3):749–69.
[6] Husain A, Hamielec AE. J Appl Polym Sci 1978;22(5):1207–23.
[7] Marten FL, Hamielec AE. In: Henderson JN, Bouton TC, editors. Polymerization reactors and processes. Am Chem Soc Symp Ser, 104, 1979. p. 43–69.
[8] Hamielec AE. Chem Eng Commun 1983;24:1–19.
[9] Cardenas JN, O' Driscoll KF. J Polym Sci, Polym Chem Ed 1976; 14(4):883–97.
[10] Mahabadi HK, O' Driscoll KF. Macromolecules 1977;10(1):55–8.
[11] O' Driscoll KF. Pure Appl Chem 1981;53(3):617–26.
[12] Schmidt AD, Ray WH. Chem Eng Sci 1981;36(8):1401–10.
[13] Tulig TJ, Tirrell M. Macromolecules 1981;14(5):1501–11.
[14] Soh SK, Sundberg DC. J Polym Sci, Polym Chem Ed 1982;20(5): 1299–313.
[15] Soh SK, Sundberg DC. J Polym Sci, Polym Chem Ed 1982;20(5): 1315–29.
[16] Soh SK, Sundberg DC. J Polym Sci, Polym Chem Ed 1982;20(5): 1331–44.
[17] Soh SK, Sundberg DC. J Polym Sci, Polym Chem Ed 1982;20(5): 1345–71.
[18] Chiu WY, Carratt GM, Soong DS. Macromolecules 1983;16(3): 348–57.
[19] Mita I, Horie K. JMS-Rev Macromol Chem Phys 1987;C27(1): 91–169.
[20] Achilias DS, Kiparissides C. J Appl Polym Sci 1988;35(5):1303–23.
[21] Achilias DS, Kiparissides C. Macromolecules 1992;25(14):3739–50.
[22] Keramopoulos A, Kiparissides C. Macromolecules 2002;35(10): 4155–66.
[23] Russell GT, Napper DH, Gilbert RG. Macromolecules 1988;21(7): 2133–40.
[24] Russell GT, Napper DH, Gilbert RG. Macromolecules 1988;21(7): 2141–8.
[25] Russell GT, Gilbert RG, Napper DH. Macromolecules 1992;25(9): 2459–69.
[26] Russell GT, Gilbert RG, Napper DH. Macromolecules 1993;26(14): 3538–52.
[27] Russell GT. Macromol Theor Simul 1995;4(3):497–517.
[28] Russell GT. Macromol Theor Simul 1995;4(3):519–48.
[29] Russell GT. Macromol Theor Simul 1995;4(3):549–76.
[30] Clay PA, Gilbert RG, Russell GT. Macromolecules 1997;30(7): 1935–46.
[31] Zhu S. Macromolecules 1996;29(1):456–61.
[32] Beuermann S, Buback M, Davis TP, Gilbert RG, Hutchinson RA, Olaj OF, Russell GT, Schweer J, Van Herk AM. Macromol Chem Phys 1997;198(5):1545–60.
[33] O'Neil GA, Wisnudel MB, Torkelson JM. Macromolecules 1996; 29(23):7477–90.
[34] O'Neil GA, Wisnudel MB, Torkelson JM. Macromolecules 1998; 31(14):4537–45.
[35] O'Neil GA, Torkelson JM. Macromolecules 1999;32(2):411–22.
[36] Qin J, Guo W, Zhang Z. Polymer 2002;43(4):1163–70.
[37] Qin J, Li H, Zhang Z. Polymer 2003;44(8):2599–604.
[38] Willemse RXE, Staal BBP, Van Herk AM, Pierik SCJ, Klumperman B. Macromolecules 2003;36(26):9797–803.
[39] de Gennes PG. J Chem Phys 1971;55(2):572–9.
[40] de Gennes PG. Macromolecules 1976;9(4):587–93.
[41] de Gennes PG. Macromolecules 1976;9(4):594–8.
[42] de Gennes PG. Nature (London) 1979;282:367–70.
[43] Vrentas JS, Duda JL. J Polym Sci Polym Phys 1977;15(3):403–16.
[44] Vrentas JS, Duda JL. J Polym Sci Polym Phys 1977;15(3):417–39.
[45] Ray WH. J Macromol Sci Rev Macromol Chem 1972;C8(1):1–56.
[46] Arriola DJ. Modeling of addition polymerization systems. PhD Thesis. University of Wisconsin, USA; 1989.
[47] Achilias DS, Kiparissides C. J Macromol Sci Rev Macromol Chem 1992;C32(2):183–234.
[48] Verros G, Papadakis M, Kiparissides C. Polym React Eng 1993;1(3): 427–60.
[49] Kiparissides C, Verros G, MacGregor JF. JMS-Rev Macromol Chem Phys. 1993;C33(4):437–527.
[50] Flory PJ. Principles of polymer chemistry. Ithaca: Cornell University Press; 1953.
[51] Stockmayer WH. J Chem Phys 1943;11(2):45–55.
[52] Simha R, Branson H. J Chem Phys 1944;12(6):253–67.
[53] Tobita H. Macromolecules 1993;26(4):836–41.
[54] Tobita H. Polymer 1994;35(14):3023–31.
[55] Tobita H. Polymer 1994;35(14):3032–8.
[56] Tobita H. J Polym Sci, Part B: Polym Phys 1995;33(12):1769–80.
[57] Tobita H. Macromolecules 1996;29(2):693–704.
[58] Stockmayer WH. J Chem Phys 1945;13(6):199–207.
[59] Hamielec AE, Hodgins JW, Tebbens K. AIChE J 1967;13(6): 1087–91.
[60] Hamielec AE, MacGregor JF, Penlidis A. Makromol Chem Macromol Symp 1987;10/11:521–70.
[61] Tobita H, Hamielec AE. Macromolecules 1989;22(7):3098–105.
[62] Xie T, Hamielec AE. Macromol Theor Simul 1993;2(3):455–83.
[63] Cunningham BF, Mahabadi HK. Macromolecules 1996;29(3): 835–41.
[64] Fiorentino S, Ghielmi A, Storti G, Morbidelli M. Ind Eng Chem Res 1997;36(4):1283–301.
[65] Ray WH. Macromolecules 1971;4(2):162–5.
[66] Ray WH, Douglas TL, Godsalve EW. Macromolecules 1971;4(2): 166–74.
[67] Nagasubramanian K, Graessley WW. Chem Eng Sci 1970;25(10): 1549–58.
[68] Tobita H, Ito K. Polym React Eng 1992/1993;1(3):407–25.
[69] Crowley TJ, Choi KY. Ind Eng Chem Res 1997;36(5):1419–23.
[70] Yoon WJ, Ryu JH, Cheong C, Choi KY. Macromol Theor Simul 1998;7(3):327–32.
[71] Teymour F, Campbell JD. Macromolecules 1994;27(9):2460–9.
[72] Maschio G, Scali C. Macromol Chem Phys 1999;200(7):1708–21.
[73] Liu SL, Amundson NR. Rubber Chem Technol 1961;34:995–1133.
[74] Detar DF, Detar CE. J Phys Chem 1966;70(12):3842–7.
[75] Verros GD. Polymer 2003;44(22):7021–32.
[76] Zeman R, Amundson NR. Chem Eng Sci 1965;20(4):331–61.
[77] Zeman R, Amundson NR. Chem Eng Sci 1965;20(7):637–64.
[78] Coyle DJ, Tulig TJ, Tirrell M. Ind Eng Chem Fundam 1985;24(3): 343–51.

[79] Ellis MF, Taylor TW, Gonzalez V, Jensen KF. AIChE J 1988;34(8):1341–53.
[80] Bailagou PE, Soong DS. Chem Eng Sci 1985;40(1):87–104.
[81] Chaimberg M, Cohen Y. Ind Eng Chem Res 1990;29(7):1152–60.
[82] Gonzalez-Romero VM, Rodriguez BE. Chem Eng Commun 1987;59:185–200.
[83] Budde U, Wulkow M. Chem Eng Sci 1991;46(2):497–508.
[84] Canu P, Ray WH. Comput Chem Eng 1991;15(8):549–64.
[85] Wulkow M. Macromol Theor Simul 1996;5(3):393–416.
[86] Russell GT. Aust J Chem 2002;55:399–414.
[87] Biesenberger JA, Sebastian DH. Principles of polymerization engineering. New York: Wiley-Interscience; 1987.
[88] North AM. Makromol Chem 1965;83(1):15–22.
[89] Smoluchowski M. Z Phys Chem 1918;92:129–68.
[90] Parker TS, Chua LO. Practical numerical algorithms for chaotic systems. New York: Springer; 1989.
[91] Press WH, Teukolsky SA, Vetterling WT, Flannery BP. Numerical recipies in Fortran 77 the art of scientific computing. 2nd ed. Fortran numerical recipies. vol. 1. New York: Cambridge University Press; 1992.
[92] Jones KM, Bhattacharya D, Brash JL, Hamielec AE. Polymer 1986;27(4):602–10.
[93] Bhattacharya D, Hamielec AE. Polymer 1986;27(4):611–8.
[94] Yaraskavitch IM, Brash JL, Hamielec AE. Polymer 1987;28(3):489–96.
[95] Chiantore O, Hamielec AE. Polymer 1985;26(4):608–14.
[96] Bamford CH, Tompa H. Trans Faraday Soc 1954;50:1097–116.
[97] Balke ST, Hamielec AE. J Appl Polym Sci 1973;17(3):905–49.
[98] Zhu S, Tian Y, Hamielec AE, Eaton DR. Polymer 1990;31(1):154–9.
[99] Verros GD, Malamataris NA. Ind Eng Chem Res 1999;38(9):3572–80.
[100] Verros GD, Malamataris NA. Macromol Theor Simul 2001;10(8):737–49.
[101] Ju ST, Duda JL, Vrentas JS. Ind Eng Chem, Prod Res Dev 1981;20(2):330–5.
[102] Ju ST, Liu HT, Duda JL, Vrentas JS. J Appl Polym Sci 1981;26(11):3735–44.